

# Energy potential of pumps as turbines (PATs) in water distribution networks

*Mauro Venturini\**, *Stefano Alvisi*, *Silvio Simani*

*Dipartimento di Ingegneria, Università degli Studi di Ferrara, Ferrara (Italy),*

*mauro.venturini@unife.it, stefano.alvisi@unife.it, silvio.simani@unife.it*

*\* Corresponding author*

## **Abstract:**

This paper deals with the estimation of the energy potential of pumps used as turbines to exploit residual hydraulic energy, as in the case of available head and flow rate in water distribution networks.

To this aim, four pumps with different characteristics are investigated to estimate the producible yearly electric energy. The performance curves of Pumps As Turbines (PATs), which relate head, power and efficiency to the volume flow rate over the entire PAT operation range, were derived by using published experimental data. The three considered water distribution networks, for which experimental data taken during one year were available, are characterized by significantly different hydraulic features (average flow rate in the range 10 – 116 l/s; average pressure reduction in the range 12 - 53 m). Therefore, energy potential estimation accounts for actual flow rate and head variability over the year. The conversion efficiency is also estimated, for both the whole water distribution network and the PAT alone. Finally, a rule of thumb is established in order to select the optimal pump to be used as a PAT, as a function of the characteristics of the considered water distribution network.

The results presented in this paper can be used as a guideline for a preliminary evaluation of energy and economic feasibility of PATs aimed to exploit the hydraulic energy potential of water distribution networks.

## **Keywords:**

Pump As Turbine; Pump; Water Distribution Network; Hydraulic Energy; Efficiency.

## **1. Introduction**

To a greater or lesser extent, all water distribution networks (WDNs) are affected by leakages [1]; these leakages cause economic losses and environmental concerns due to the amount and cost of lost water and energy consumed by pumping stations, which must handle larger volumes of water than those effectively delivered to the users [2]. The rate of water losses in a leaking pipe of a water distribution system is strictly related to the pressure value [1,3]: the higher the pressure, the larger the water volume lost. Therefore, pressure control strategies should be adopted to minimize excessive pressures as far as possible, while ensuring sufficient pressures to satisfy customer demands at all times. As the complexity of a water distribution system grows, the task of achieving the optimal target pressure level becomes more difficult [4].

Operatively, pressure control in WDNs can be achieved by creating district metered areas [5] and/or placing pressure reducing valves (PRVs) [6] to prevent the downstream hydraulic pressure from exceeding the desired value. PRVs are variable closure devices that reduce the conveyance capacity of the pipe by increasing the pressure losses [4]. Therefore, at present, the number of PRVs is increasing in real WDNs and, in the framework of a virtuous energy policy, any attempt should also be made by water network managers to convert energy dissipation into energy production [7].

The theoretical convertible power is considerable and could lead to large energy savings; for instance, according to some recent studies, it may be in the order of 4.7 MW in Germany [7] or about 17 MW in UK water industry [8]. Nevertheless, energy production in water supply systems

has been realized only in few cases and mainly in the transmission pipelines, where the available hydraulic power is considerable and fairly constant. Conversely, the dissipation nodes in urban WDNs usually present a large variability in flow rate and head drop and thus sustainable energy production within WDNs still represents an open challenge.

As highlighted in [9], among the different turbines that can be coupled with low and variable power, Pump As Turbines (PATs) can be considered a good alternatives, since they combine low installation costs with an acceptable energy production. Indeed, pumps can be used in turbine mode by reversing flow direction with the engine acting as a generator [10]. The use of PATs may also increase WDN flexibility, e.g. by changing PAT working conditions in case of pipe failure.

One of the main challenges is that pump manufactures do not usually provide the performance curves of pumps in reverse operation and the designer should face a lack of data that constitutes an obstacle to the choice of the most suitable machine. Therefore, establishing a correlation that enables the transfer from “pump” characteristics into “turbine” characteristics is crucial. Many researchers have presented some theoretical and empirical relationships for predicting PAT characteristics for the Best Efficiency Point (BEP) [11-14], while so far a procedure to estimate their performance in turbine mode over the entire operation range is not completely established in literature. In fact, experimental characterization is usually required case by case.

In this framework, this paper evaluates the energy potential of four different PATs (characterized by means of experimental performance curves) installed in three different WDNs (also characterized by means of experimental data). The result of the analysis is the estimation of the producible electric energy and the corresponding conversion efficiency from the available hydraulic energy, with the final goal of identifying a rule of thumb for maximizing the producible electric energy.

Therefore, this paper is organized as follows. Pump and PAT performance curves are presented in Section 2; the main characteristics of the real case WDNs are provided in Section 3; the results of the analysis of PATs’ energy potential for the considered case studies are presented and discussed in Section 4; finally conclusions are provided.

## **2. Pump and PAT performance**

### **2.1 – Available field data from literature**

The starting point for deriving pump and PAT performance curves over the entire range of operation is the paper [11], authored by Derakhshan and Nourbakhsh. The authors reported the performance data taken experimentally on four different turbomachines, running in both pump and PAT mode. The four pumps are characterized by  $\Omega$  values in the range 1.53 - 5.82.

The pump characteristic values at the respective BEP are reported in Table 1. These values are calculated in this paper by considering that the experimental non-dimensional data reported in [11] were taken at  $n$  equal to 25 rps (i.e. 1500 rpm) and pump nominal diameter  $D$  was equal to 0.25 m.

It can be seen that the four pumps are characterized by considerably different values of power, from about 3 kW to about 22 kW. Accordingly, the volume flow rate at BEP passes from 8.0 l/s to 107.7 l/s and the maximum efficiency increases from 64.5% to 86.8%. Otherwise, the head at BEP decreases from 24.9 m to 18.3 m, passing from pump #1 to pump #4.

Table 2 reports the operating ranges of the four pumps/PATs. It can be seen that the four considered pumps can swallow up to 148 l/s (pump #4), with a maximum head of 29 m (pump #1), maximum power consumption of about 25 kW and maximum efficiency of 87% (both maximum power and maximum efficiency values refer to pump #4).

Table 1. Pump characteristics at BEP (\* Reported in [11];\*\* Estimated through Eq. (1);\*\*\* Calculated as  $\rho \cdot Q \cdot g \cdot H / \eta$ )

Pump	$\Omega^*$ , -	$Q^*$ , $10^{-3} \text{ m}^3/\text{s}$	$\eta^*$ , %	$H^{**}$ , m	$P^{***}$ , W
#1	1.53	8.0	64.5	24.9	3044
#2	2.41	24.8	75.7	22.1	7114
#3	3.94	62.2	86.3	21.1	14,926
#4	5.82	107.7	86.8	18.3	22,288

Table 2. Pump and PAT operating range reported in [11]

Pump	$Q$ , $10^{-3} \text{ m}^3/\text{s}$	$H$ , m	$P$ , W	$\eta$ , %
#1	0.0 – 12.7	15.3 – 29.2	1559 – 2525	40.1 – 64.5
#2	0.0 – 43.9	10.9 – 24.7	4084 – 9504	30.0 – 75.7
#3	0.0 – 94.4	12.5 – 25.5	8465 – 18,860	30.3 – 86.3
#4	0.0 – 148.3	12.4 – 23.1	14,405 – 24,800	30.0 – 86.8
PAT	$Q$ , $10^{-3} \text{ m}^3/\text{s}$	$H$ , m	$P$ , W	$\eta$ , %
#1	10.4 – 18.3	27.0 – 67.7	668 – 4752	24.8 – 63.1
#2	19.5 – 43.5	19.8 – 50.8	817 – 15,296	25.1 – 71.6
#3	31.5 – 95.9	15.4 – 38.7	0 – 26,582	0.0 – 74.7
#4	55.2 – 129.3	12.1 – 27.1	0 – 25,468	0.0 – 78.3

Instead, the maximum volume flow rate allowed for PAT operation is slightly lower than that of the pump (i.e. up to 129 l/s for PAT #4). The required head is rather different for the four PATs, e.g. it is in the range 27 m – 68 m for PAT #1 and 12 m – 27 m for PAT #4. The maximum producible electric power passes from less than 5 kW (PAT #1) to more than 25 kW (PAT #4). Moreover, the maximum value of efficiency in PAT mode is lower than the maximum efficiency in pump mode.

## 2.2 –Pump and PAT performance curves

In this paper, pump and PAT behavior was modelled independently, by interpolating the available experimental data reported in [11]. A functional dependence by means of a second-order, third-order and fourth-order polynomial was investigated. The second-order polynomial functions proved the best fit for all the non-dimensional parameters  $Y$ , both for the pump and the PAT, according to Equations (1) and (2) respectively. This representation also allows a physically consistent modeling over the entire range of operation.

$$Y_p(\Omega, \phi) = a_{2p}(\Omega) \cdot \phi^2 + a_{1p}(\Omega) \cdot \phi + a_{0p}(\Omega) \quad (1)$$

$$Y_{PAT}(\Omega, \phi) = a_{2PAT}(\Omega) \cdot \phi^2 + a_{1PAT}(\Omega) \cdot \phi + a_{0PAT}(\Omega) \quad (2)$$

The interpolation curves expressed in Equations (1) and (2) are reported in Figures 1a, 1b and 1c. In these figures, the non-dimensional flow rate is assumed positive, for both the pump and the PAT.

To assess the prediction reliability of the selected modeling approach, the Root Mean Square Error  $RMSE_{Yk}$ , expressed in Equation (3), is adopted:

$$RMSE_{Yk} = \sqrt{\frac{1}{N} \sum_{i=1}^N \left( \frac{(Y_{ki})_e - (Y_{ki})_s}{(Y_{ki})_e} \right)^2} \quad Y = \psi, \pi, \eta; k = 1, 2, 3, 4 \quad (3)$$

The index defined in Equation (3) compares each experimental value of the performance parameter  $(Y_{ki})_e$  for a given turbomachine  $k$  (both in pump and PAT mode) to the corresponding simulated value  $(Y_{ki})_s$ , predicted by means of Equations (1) and (2).

The values of  $RMSE_{Y_k}$  are summarized in Figure 2. It can be noticed that, in general,  $RMSE_{\psi}$  values are very good in both pump and PAT mode (they are in the range 0.5% - 2.6%). Moreover,  $RMSE_{\pi}$  values in pump mode are even better (values in the range 0.2% - 1.6%). Otherwise,  $RMSE_{\pi}$  values in PAT mode are considerably higher (values in the range 1.9% - 7.5%) and this also reflects on the values of  $RMSE_{\eta}$ . However, the selected interpolating functions expressed in Equations (1) and (2) are considered satisfactory for the purpose of this paper, since they provide a physics-responding approach for simulating the behavior of pumps and PATs over the entire range of operation.

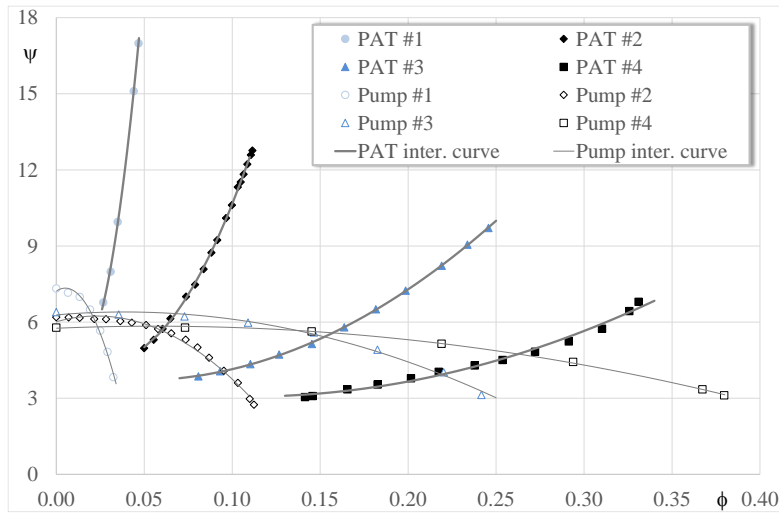


Fig. 1a. Non-dimensional head vs. non-dimensional volume flow rate (symbols: experimental data reported in [11]; lines: interpolation curves).

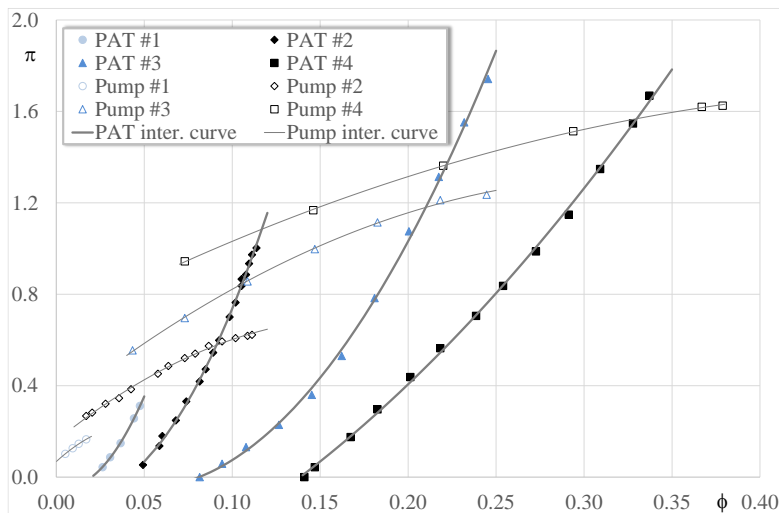


Fig. 1b. Non-dimensional power vs. non-dimensional volume flow rate (symbols: experimental data reported in [11]; lines: interpolation curves).

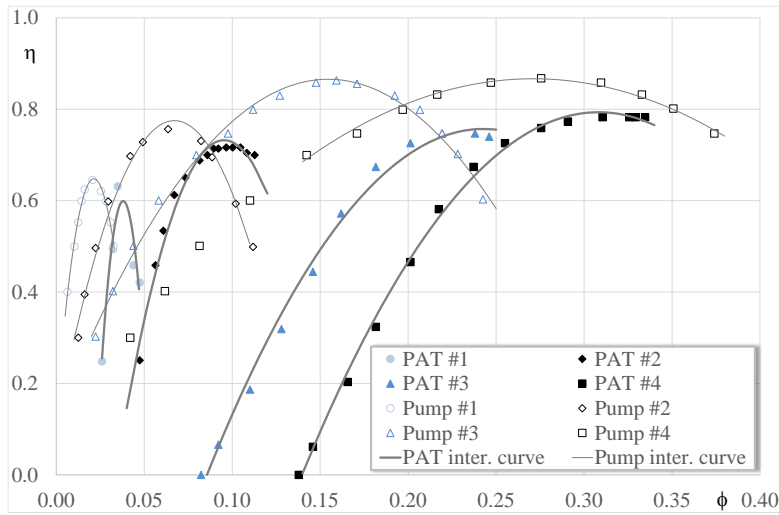


Fig. 1c. Efficiency vs. non-dimensional volume flow rate (symbols: experimental data reported in [11]; lines: interpolation curves).

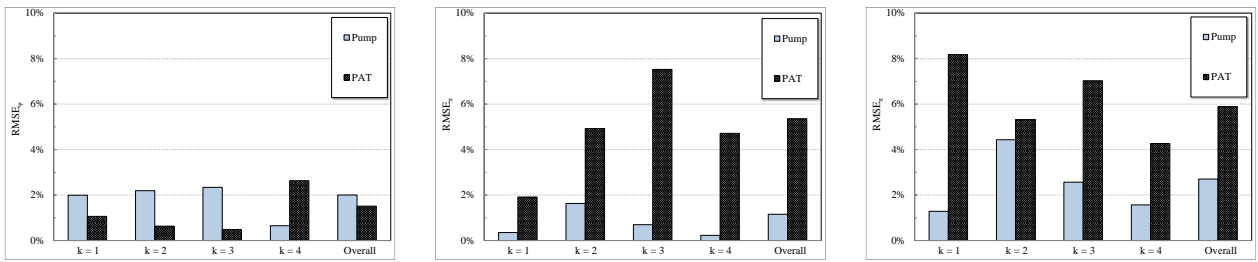


Fig. 2.  $RMSE_{Y_k}$  values for non-dimensional head (left), non-dimensional power (center) and efficiency (right).

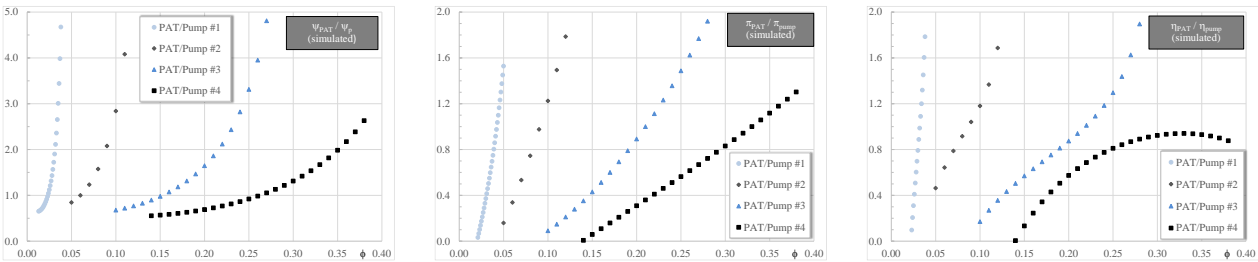


Fig. 3. Ratio function  $R$  for non-dimensional head (left), non-dimensional power (center) and efficiency (right).

Finally, differently from other approaches followed in literature (e.g., the functional dependence in [11] is related to the flow rate at BEP), by using the relationships established in Equations (1) and (2), the ratio function  $R$  is calculated according to Equation (4), as the ratio between the non-dimensional parameter  $Y$  ( $\psi$ ,  $\pi$  or  $\eta$ ) in PAT mode and the same non-dimensional parameter in pump mode at a given non-dimensional volume flow rate, for all the pumps/PATs (#1 through #4):

$$R(\Omega, \phi) = Y_{PAT}(\Omega, \phi) / Y_P(\Omega, \phi) \quad (4)$$

The ratio functions  $R$  reported in Figure 3 allow to relate PAT's performance curves to pump's performance curves, for each considered specific speed. Moreover, by using the data in Figure 3, it is possible to estimate PAT's performance at any working point if pump performance at a given working point (not necessarily the BEP) is known, for  $\Omega$  values in the range 1.53 - 5.82.

### 3. Field data of water distribution networks

#### 3.1 – Water distribution networks

The three water distribution networks (WDN A, B and C) considered in this paper are located in Italy. WDN A and WDN B serve two small towns, featuring around 950 and 2100 users respectively. WDN C serves a part of a large city, featuring around 8500 users. The total length of each system is about 45 km, 102 km and 150 km for WDN A, B and C, respectively.

The three WDNs lay at the foot of a hill zone and are fed by the same water supply system, as shown in Figure 4. In particular, each WDN is connected to the water main in just one point; a PRV is currently located at each connection point in order to reduce the downstream pressure since the pressure within the water main is considerably higher than that required within the distribution system. Indeed, within each WDN, the pressure is fixed at around 35 m, while the pressure within the main varies from around 80-90 m (next to WDN A and B which are located in the lowest part of the served area) to around 45 m (next to WDN C, which is located in the highest part of the served area). Consequently the head drop is considerably larger at the PRVs located at the inlet point of WDN A and B, whereas it is lower at the PRV located at the inlet point of WDN C.

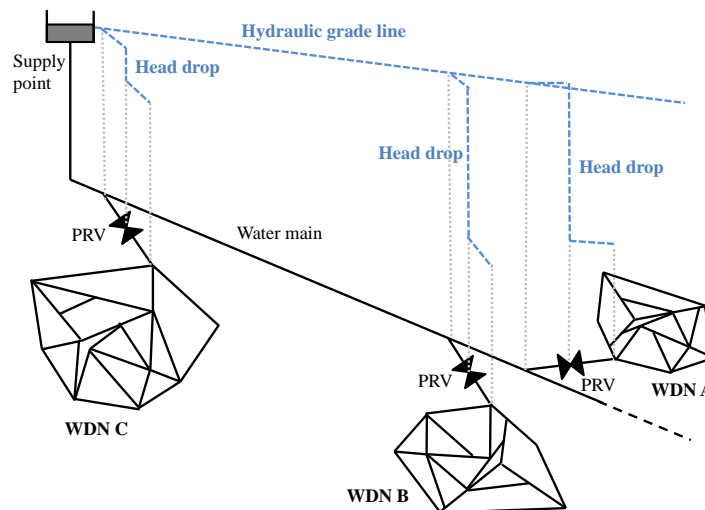


Fig. 4. Layout of the three WDNs.

As discussed in the Introduction, such a layout allows an effective pressure control within the network, leading to significant benefits in terms of leakage reduction. On the other hand, a significant amount of energy is currently wasted in correspondence of each PRV.

#### 3.2 – Available field data

The available field data were taken over one year (year 2013), every 15 minutes. Therefore, 35,040 measured data sets are available per each WDN. Each data set consists of two measured parameters: the volume flow rate  $Q$  and the head drop  $H$ . All the available field data are shown in Figure 5, while Figure 6 reports the main characteristics of the three WDNs.

According to Figure 5, WDN A and B are characterized by similar values of head drop at the inlet point (roughly in the range 20 m – 80 m), while WDN C has a significantly lower average head drop at the inlet point (roughly in the range 5 m – 15 m). Instead, according to Figure 6, the average volume flow rate changes dramatically from WDN A (10 l/s) to WDN C (116 l/s), while it is 28 l/s for WDN B. Moreover, several peak values of head drop were measured in WDN A (up to about 90 m) in correspondence of the smallest values of the volume flow rate. Otherwise, WDN C is characterized by almost regular values of head drop (average value equal to 12 m), but the volume flow rate is usually considerably higher than that of WDN A and B (mean value: 116 l/s; maximum

value: 292 l/s). Therefore, the three WDNs are representative of different scenarios, which challenge the installation of a PAT to a different extent.

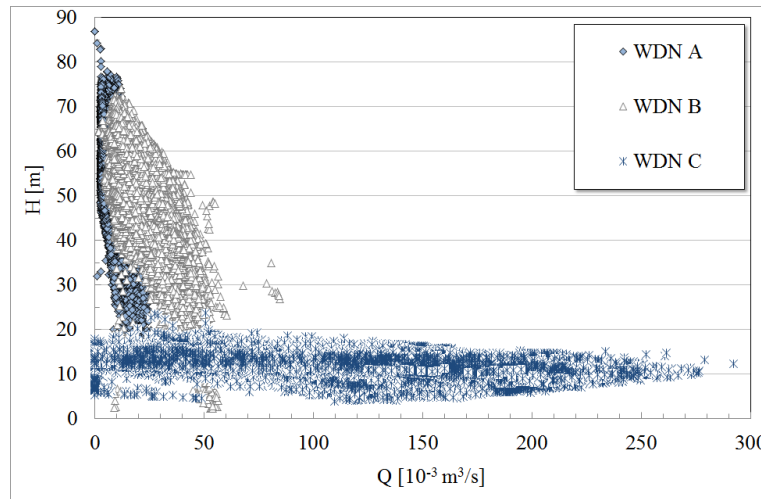


Fig. 5. Available head drop vs. volume flow rate (measured values).

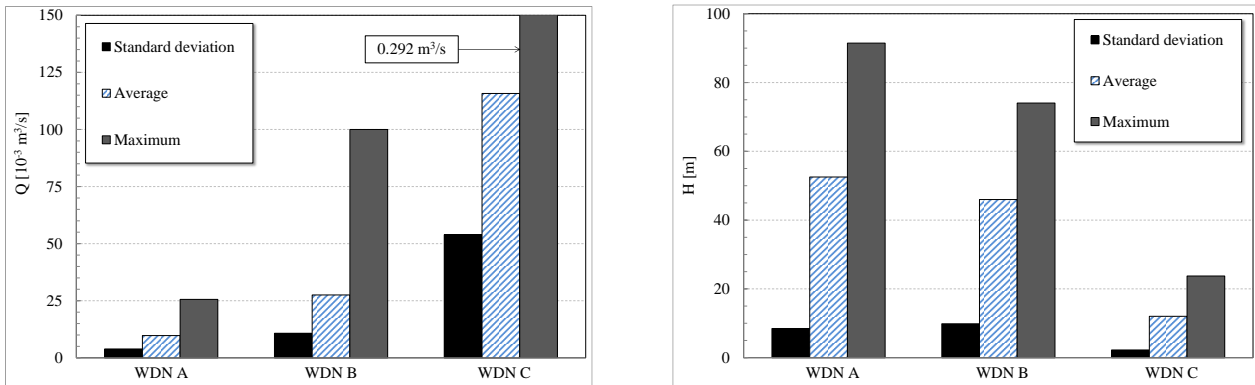


Fig. 6. Summary of volume flow rate and head drop for WDN A, B and C.

## 4. Analysis of PAT's potential

The aim of the analysis reported in this section is threefold:

1. Assessment of the energy potential of otherwise-wasted hydraulic energy. The yearly producible electric energy is obtained by considering the actual PAT working point for each data set. The working point is set by acting on two valves, as outlined in Section 4.1;
2. Estimation of the conversion efficiency of energy recovery, for both the entire WDN (overall efficiency) and for the PAT alone (PAT efficiency);
3. Identification of a tentative rule of thumb for the optimal matching between a WDN and a pump, operated as a PAT.

### 4.1 – Energy potential

The procedure adopted to evaluate the energy potential of a PAT consists of the steps reported below:

1. Availability of pump performance curves over the entire range of operation. In this paper, four pumps (#1 through #4) are evaluated;
2. Estimation of PAT's performance curves over the entire range of operation, by using the ratio functions R defined in Equation (4) and shown in Figure 3;

3. Estimation of the producible electric power for each data set (i.e. for each time point), by considering that:
  - a. If  $H_{PAT} \leq H_{meas}$ , the producible electric power is calculated at  $Q_{meas}$  and  $H_{PAT}$ . This means that there is a reduction of  $H$ , so that  $\Delta H_{un} = H_{meas} - H_{PAT}$  is unexploited. In other words, available head has to be dissipated;
  - b. If  $H_{PAT} > H_{meas}$ , the producible electric power is calculated at  $Q_{thr}$  (lower than  $Q_{meas}$ ) and  $H_{meas}$ . In fact, the volume flow rate flowing through the PAT has to be decreased, so that, in this case,  $Q_{un} = Q_{meas} - Q_{thr}$  is unexploited;
4. Calculation of the producible electric energy by multiplying the producible electric power by the sampling time of WDN data (in this paper, 15 minutes);
5. Calculation of the producible electric energy over one year.

As it can be observed, the regulation system is assumed in this paper as simple as possible to lower both installation and operation costs. In fact, it is composed of only two valves: one valve in series with the PAT, to dissipate the excess pressure/head, and one valve in parallel (bypass valve), which can be opened to reduce the volume flow rate through the PAT to the value that makes  $H_{PAT}$  equal to  $H_{meas}$ . This regulation strategy was also discussed and investigated in [15] (where it was identified as “hydraulic regulation”) and represents a feasible operation mode for WDNs. It is clear that the possibility of varying PAT’s rotational speed and consequently moving PAT’s characteristic curve in order to match, at each time point, the available head and flow rate, may increase the producible electric energy, but would require the use of an inverter and a more sophisticated regulation system. This option is not considered in this paper and will be investigated separately by the authors, by also considering system transient behavior, as made in [16].

The producible yearly electric energy, estimated according to the procedure outlined above, is reported in Figure 7. It can be seen that, for all the three WDNs, an optimal solution which is by far preferable with respect to other possible combinations can be identified, i.e. PAT #1 for WDN A, PAT #2 for WDN B and PAT #4 for WDN C. This is clearly due to the matching of PAT’s performance curves (see Figure 1) and WDN characteristics (see Figures 5 and 6). The value of the maximum producible yearly electric energy is almost comparable for WDN A and WDN C (6650 kWh and 9548 kWh, respectively), while it is considerably higher for WDN B (40,036 kWh). In fact, on average, the WDN B is characterized by a combination of higher flow rate and head (see Figure 5). However, it can be noted that, in all combinations, the producible yearly electric energy is rather low. For instance, the producible yearly electric energy can be compared to the residential electricity consumption per capita in 2010 in the EU-27, which was equal to 1682 kWh [17]. Thus, in the best case, the electric energy demand of only twenty-four household users can be met.

The energy potential which cannot be exploited is reported in Figure 8, only for the three best combinations of WDN/PAT. It can be seen that the two solutions WDN A / PAT #1 and WDN B / PAT #2 are similar, i.e. available head is usually wasted. Otherwise, for the solution WDN C / PAT #4, a considerable amount of volume flow rate is always unexploited (at least 100 l/s). These results are coherent with the considered installation scheme and regulation system, which makes use of two valves dissipating excessive pressure and flow rate at fixed rotational speed. Indeed, larger amount of available head and volume flow rate could be exploited by considering an electrical regulation of the rotational speed, even though recent studies pointed out that the latter approach is, on the whole, less efficient and convenient than the former [18].



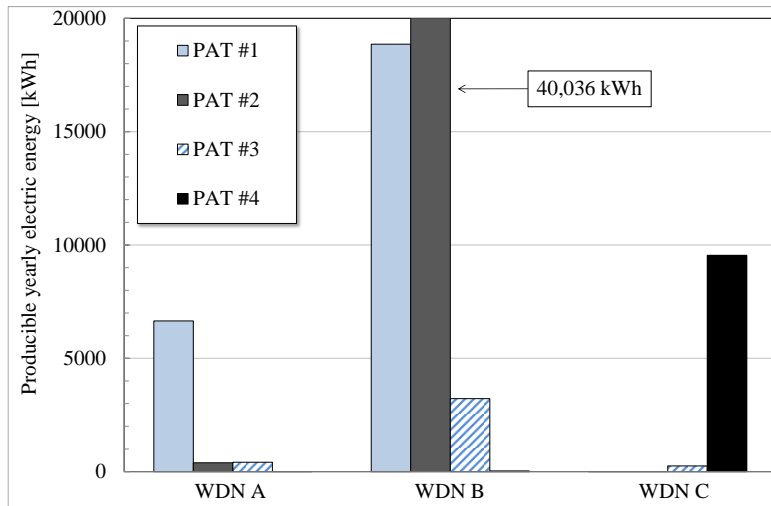


Fig. 7. Producibility yearly electric energy.

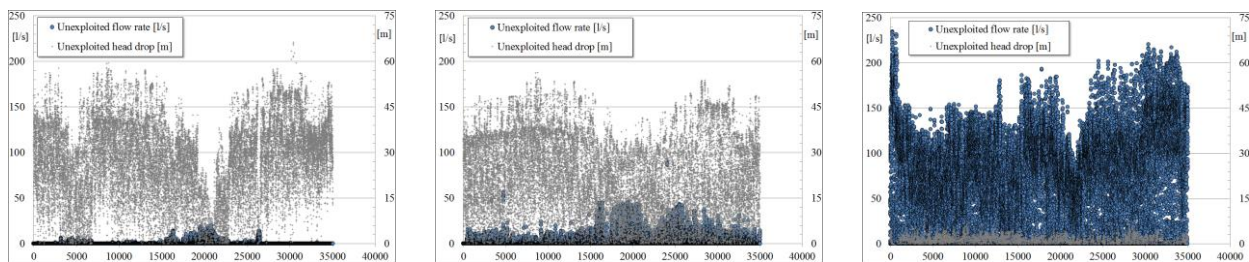


Fig. 8. Unexploited flow rate and head drop for WDN A and PAT #1 (left), WDN B and PAT #2 (center) and WDN C and PAT #4 (right).

## 4.2 – Conversion efficiency

The estimation of the conversion efficiency is carried out by considering both the energy potential from the whole WDN (i.e. available flow rate and head) and PAT internal efficiency. In fact, the former conversion efficiency (overall efficiency) accounts for the incomplete exploitation of flow rate and head observed in Figure 8, while the latter (PAT efficiency) accounts for the fact that the producible electric energy was calculated by considering the *actual* operating point per each data set (i.e. per each available time point), which, in general, can be considerably far from the BEP.

The results of this analysis are summarized in Figure 9. From an overall perspective (see Figure 9 on the left), the WDN potential is usually rather unexploited, with the exception of one case (WDN B and PAT #2) that has an overall conversion efficiency of 39%. This result is in agreement with a similar analysis carried out in [15] by considering several WDNs: in fact, it was found out in [15] that only in few cases the overall efficiency was higher than 40%, while in other few cases it was only about 10%. This obviously demonstrates that the pump to be used as a PAT has to be carefully selected according to the considered WDN. On the other hand, the PAT itself usually runs with an “acceptable” efficiency (see Figure 9 on the right), if it is considered that this type of machine is not designed to work as an expander. The best case is given once again by the PAT #2 installed in the WDN B, which has a yearly average efficiency of 59%.

Another relevant achievement of this analysis is that the estimation of the producible yearly electric energy cannot be made by using all-inclusive values of overall/PAT efficiency. In fact, PAT actual working point is usually considerably far from BEP (see values in Table 2) and therefore the estimate carried out by considering BEP values would result considerably overestimated. Instead, the values provided in Figure 9, though valid only for the considered WDNs, can be used as an indication for evaluating PAT energy and economic actual potential.

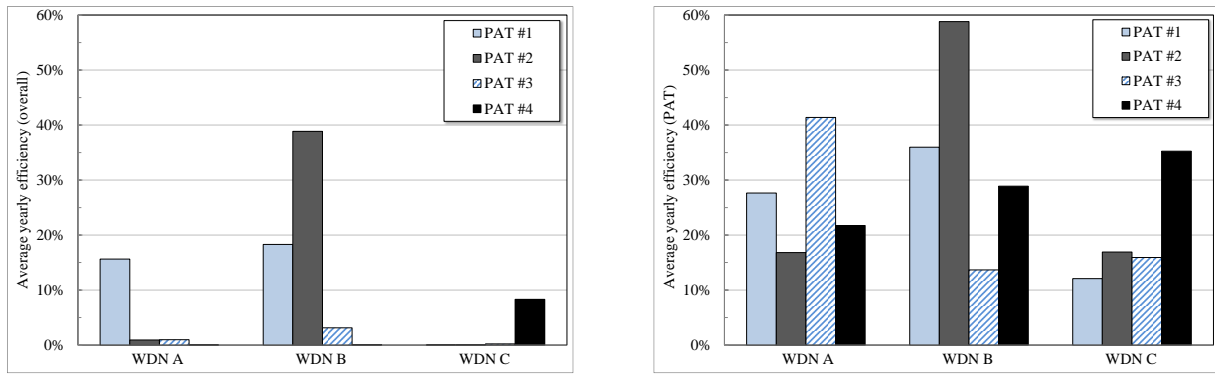


Fig. 9. Average yearly conversion efficiency: overall (left) and PAT (right).

### 4.3 – Selection of the optimal PAT

This section aims to generalize the results previously obtained, in order to provide a guideline for the selection of the most suitable pump to be used as a PAT for a given installation (in this paper, a WDN). For this purpose, the average volume flow rate (measured on the considered WDN) is scaled to the volume flow rate at BEP (one different value per each pump). As a consequence, a non-dimensional coordinate  $(Q_{\text{meas}})_{\text{av}}/Q_{\text{BEP}}$  can be calculated. Similarly, head can be scaled to calculate a non-dimensional coordinate  $(H_{\text{meas}})_{\text{av}}/H_{\text{BEP}}$ .

Figure 10 reports eleven out of the twelve considered combinations of WDN/pump; in fact, the combination WDN C – pump #1 is out of scale, since  $(Q_{\text{meas}})_{\text{av}}/Q_{\text{BEP}} = 14.4$  while  $(H_{\text{meas}})_{\text{av}}/H_{\text{BEP}} = 0.5$ .

It can be seen that all the three most preferable combinations of WDN/pump are characterized by  $(Q_{\text{meas}})_{\text{av}}/Q_{\text{BEP}}$  values very close to one. This means that the pump, when used as a PAT, can fully exploit the available flow rate, though it has to be observed that  $(Q_{\text{meas}})_{\text{av}}$  is a yearly-averaged value.

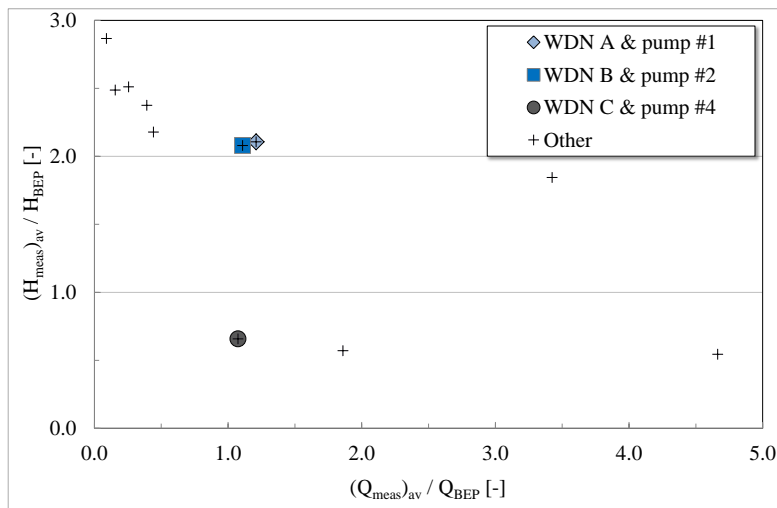


Fig. 10. Relationship between WDN average features and pump characteristics at BEP.

Moreover, the most preferable combinations of WDN and PAT are characterized by  $(H_{\text{meas}})_{\text{av}}/H_{\text{BEP}}$  values in the range 0.7 – 2.1. In fact, if  $(Q_{\text{meas}})_{\text{av}}/Q_{\text{BEP}}$  is lower or higher than one,  $(H_{\text{meas}})_{\text{av}}/H_{\text{BEP}}$  is higher than 2 or lower than 0.7, respectively. This can be explained by considering that, in general, it is preferable to have an “excess” head which, if necessary, can be dissipated, while the volume flow rate of the PAT should fit the average WDN volume flow rate to be fully exploited.

Therefore, the conclusion which can be drawn from the considered twelve combinations of pumps/WDNs is that the best pump to be used as a PAT should be characterized by  $Q_{\text{meas}}/Q_{\text{BEP}}$  in the order of one, while  $H_{\text{meas}}/H_{\text{BEP}}$  should be higher than one and preferably lower than two.

## 5. Conclusions

This paper presented an energy analysis aimed to estimate the energy potential of pumps used as turbines (PATs) to exploit the available hydraulic energy of water distribution networks. Four pumps, of which the performance both as a pump and as a turbine was known from published experimental data, were tested in three water distribution networks (WDNs), of which the experimental data over one year were also available. The pumps and the WDNs were considerably different, so that the resulting matching could be considered representative of very different scenarios.

By considering the actual variability of flow rate and available head over one year, three optimal matching pump/WDN were identified and the consequent producible electric energy was estimated. The average conversion efficiency was also estimated, for both the overall system and the PAT. It was found out that from an overall perspective the WDN potential is usually rather unexploited, with the exception of one case which had a conversion efficiency of 39%. This demonstrates that the pump to be used as a PAT has to be carefully selected according to the considered WDN. In fact, the PAT itself usually runs at “acceptable” efficiency values (up to 59%). Finally, a rule of thumb was established to select the optimal pump to be used as a PAT, on the basis of the main characteristics of the considered water distribution networks. From the considered twelve combinations of pumps/WDNs, the best pump to be used as a PAT should be characterized by (i) a design flow rate close to the yearly-averaged WDN flow rate and (ii) a design head lower than twice the yearly-averaged WDN head drop. These synthetic rules will be further verified in further works by the authors by considering additional combinations of pumps/WDNs. Another future improvement envisioned by the authors is the development of a general procedure to pass from pump performance to the corresponding PAT performance over the entire operation range.

## Nomenclature

$a$	performance curve coefficient, -
$D$	pump nominal diameter, m
$g$	gravitational acceleration, $\text{m/s}^2$
$H$	head, m
$k$	label of pump/PAT, -
$n$	rotational speed, rps
$N$	number of pump/PAT experimental data, -
$P$	power, W
PAT	pump as turbine
PRV	pressure reducing valve
$Q$	volume flow rate, $\text{m}^3/\text{s}$
$R$	ratio function $Y_{\text{PAT}}/Y_{\text{p}}$ , -
RMSE	root mean square error, -
WDN	water distribution network
$Y$	non-dimensional performance parameter ( $\pi, \eta, \psi$ ), -

## Greek symbols

$\eta$	efficiency, -
$\phi$	non-dimensional volume flow rate defined as $Q/(nD^3)$ , -

$\pi$	non-dimensional power defined as $P/(\rho n^3 D^5)$ , -
$\rho$	density, kg/m <sup>3</sup>
$\psi$	non-dimensional head defined as $gH/(n^2 D^2)$ , -
$\omega$	angular velocity, rad/s
$\Omega$	specific speed defined as $\omega Q^{0.5}/(gH)^{0.75}$ , -

### Subscripts and superscripts

1,2,3,4	label of pump/PAT
av	average
BEP	best efficiency point
e	experimental
meas	measured
p	pump
PAT	PAT
s	simulated
thr	throttle
un	unexploited
Y	non-dimensional parameter

## 6. References

- [1] Alvisi S., Franchini M., Multiobjective optimization of rehabilitation and leakage detection scheduling in water distribution systems. *Water Resources Planning and Management* 2009;135(6):426–439.
- [2] Colombo A.F., Karney B.W., Energy and Costs of Leaky Pipes: Toward Comprehensive Picture. *Water Resources Planning and Management* 2002;128(6):441–450.
- [3] Araujo L., Ramos H., Coelho S., Pressure control for leakage minimisation in water distribution systems management. *Water Resources Management* 2006;20(1):133–149.
- [4] Giugni M., Fontana N. Portolano D., Energy saving policy in water distribution networks. In: *Proceedings of International Conference on Renewable Energies and Power Quality ICREPQ'09*; 2009 April 15-17; Valencia, Spain.
- [5] Alvisi S., Franchini M., A heuristic procedure for the automatic creation of district metered areas in water distribution systems. *Urban Water* 2014;11(2):137–159.
- [6] Walsky T., Bezts W., Posluzny E., Weir M., Withman B. Modeling leakage reduction through pressure control. *American Water Works Association* 2006;98(4):148–155.
- [7] Carravetta A., Del Giudice G., Fecarotta O., Ramos H., Energy Production in Water Distribution Networks: A PAT Design Strategy. *Water Resources Management* 2012;26:3947–3959.
- [8] Zakkour P., Gochin R., Lester J., Developing a sustainable energy strategy for a water utility. Part II: a review of potential technologies and approaches. *Environmental Management* 2002; 66:115–125.
- [9] Sammartano V., Arico C., Carravetta A., Fecarotta O., Tucciarelli T., Banki-michell optimal design by computational fluid dynamics testing and hydrodynamic analysis. *Energies* 2013;6:2362–2385.
- [10] Ramos H., Borga A., Pump as turbine: an unconventional solution to energy production. *Urban Water* 1999;1:261–263.

- [11] Derakhshan S ., Nourbakhsh A., Experimental Study of Characteristic Curves of Centrifugal Pumps Working As Turbines in Different Specific Speeds. *Experimental Thermal and Fluid Science* 2008;32:800–807.
- [12] Derakhshan S ., Nourbakhsh A., Theoretical, Numerical and Experimental Investigation of Centrifugal Pumps in Reverse Operation. *Experimental Thermal and Fluid Science* 2008;32:1620–1627.
- [13] Yang, S., Derakhshan S., Kong F., Theoretical, Numerical and Experimental Prediction of Pump As Turbine Performance. *Renewable Energy* 2012;48:507–513.
- [14] Derakhshan S., Kasaeian N., Optimization, Numerical, and Experimental Study of a Propeller Pump as Turbine. *Energy Resources Technology* 2014;136(1):012005.
- [15] Fecarotta O., Aricò C., Carravetta A., Martino R., Ramos H. M., Hydropower Potential in Water Distribution Networks: Pressure Control by PATs. *Water Resources Management* 2015; 29:699–714.
- [16] Simani S., Alvisi S., Venturini M., Study of the Time Response of a Simulated Hydroelectric System. *Journal of Physics: Conference Series* 2014;570:052003.
- [17] Bertoldi P., Hirl B., Labanca N., Energy Efficiency Status Report 2012. Joint Research Centre JRC 69638, Doi 10.2788/37564.
- [18] Carravetta A., Del Giudice G., Fecarotta O., Ramos H., PAT design strategy for energy recovery in water distribution networks by electrical regulation. *Energies* 2013;6:411–424.